RSC Advances

PAPER

View Article Online
View Journal | View Issue

Cite this: *RSC Adv.*, 2022, **12**, 5489

Tapping the potential of a glucosamine polysaccharide-diatomaceous earth hybrid adsorbent in the solid phase extraction of a persistent organic pollutant and toxic pesticide 4,4′-DDT from water†

Jagadeesh Kodali,[ab] Srinivas Pavuluri,[b] Balasubramanian Arunraj,[a] A. Santhana Krishna Kumar [c] and N. Rajesh *[a]

A chitosan (a glucosamine polysaccharide)-diatomaceous earth hybrid was studied for the adsorption of 4,4′-dichloro-diphenyl-trichloroethane (4,4′-DDT), a persistent organic pollutant and organochlorine pesticide compound from water. The diverse adsorption process parameters were studied and the modified adsorbent was characterized through XRD, SEM-EDX, FT-IR, XRF, BET and TGA analysis. The concentration of 4,4′-DDT was measured using gas chromatography-tandem mass spectrometry (GC-MS/MS) by adopting a validated analytical procedure. The Langmuir and Freundlich isotherms ascertained the adsorption capacity. The optimum pH and temperature for 4,4′-DDT adsorption were found to be between 5.0 and 7.0 and 20 and 30 °C respectively. Thermodynamic parameters confirmed that the adsorption of DDT on chitosan modified with diatomaceous earth was an exothermic process. The data obtained from kinetics and intra-particle diffusion showed that the composite material is able to sequester 4,4′-DDT and this is reflected in the Langmuir adsorption capacity of 0.968 mg g^{-1}. The adsorbed 4,4′-DDT was successfully eluted with ethyl acetate and recycling studies showed that the modified chitosan can be used for three cycles with significant adsorption performance and this adsorbent proved its efficacy in removing 4,4′-DDT from farm water.

Received 25th October 2021
Accepted 20th January 2022

DOI: 10.1039/d1ra07868b

rsc.li/rsc-advances

Introduction

4,4′-Dichloro-diphenyl-trichloroethane (4,4′-DDT) is an organochlorine compound, originally developed as a modern synthetic insecticide.[1] During World War II, it was employed to contain the spread of malaria and typhus.[2] Later it was promoted for use as an agricultural pesticide. DDT is toxic, environmentally hazardous, and carcinogenic.[3] Due to the stability of the carbon–chlorine bond toward hydrolysis, it is highly resistant to biological and photolytic degradation.[4] Reports indicate that DDT persists in the environment for a long time[5,6] and was identified as a persistent organic pollutant (POP) and prohibited for agricultural use in many countries.[1] Long-term exposure to DDT causes a severe impact on human health. The breakdown of persistent organic pollutants is very slow and the soil half-life for DDT ranges between 2 and 15 years while in aqueous medium it is about 150 years.[7,8] Due to its toxicity and carcinogenicity, it is essential to remove DDT from agricultural run-off water streams.[9–12] The World Health Organization (WHO) specified a 0.001 mg L^{-1} limit for DDT[13] as well as its metabolites in drinking water. The Bureau of Indian Standards (BIS), India also stipulated the acceptable limit[14] as 0.001 mg L^{-1}.

Solid-phase extraction, adsorption, ion exchange, biosorption, nano-filtration have been extensively studied for pesticide removal and among the various water treatment methods, adsorption is quite efficient for the removal of micro contaminants.[15] In the efforts towards the development of a more sustainable adsorbent, chitosan was chosen as it is relatively environment friendly and cost-effective. Chitosan is a linear polysaccharide having β-(1,4)-linked d-glucosamine (deacetyl unit) and acetyl *N*-acetyl-d-glucosamine (acetyl unit). Commercially, chitosan is obtained by the deacetylation of chitin and the biocompatibility, non-

[a]*Department of Chemistry, Birla Institute of Technology and Science, Pilani-Hyderabad Campus, Jawahar Nagar, Shameerpet Mandal, R.R. Dist 500078, India. E-mail: nrajesh@hyderabad.bits-pilani.ac.in; Fax: +91 40 66303998; Tel: +91 40 66303503*

[b]*VIMTA Labs Limited, No. 5, MN Park, Genome Valley, Shameerpet, Hyderabad 500101, India*

[c]*Department of Chemistry, National Sun Yat-Sen University, No. 70, Lien-hai Road, Gushan District, Kaohsiung 80424, Taiwan*

† Electronic supplementary information (ESI) available: Figs: 4,4′-DDT calibration curve, precursor/product ion, spectrum and peaks of blank and sample, thermogravimetric analysis, UV spectrum of 4,4′-DDT, XRD of chitosan-diatomaceous earth adsorbent, MS-spectrum, fragmentation of 4,4′-DDT. Tables: adsorbent regeneration, impact of varying pesticides and application to farm water. See DOI: 10.1039/d1ra07868b

toxicity and biodegradability enables chitosan an appealing adsorbent.[16–19] Primary amino and hydroxyl groups facilitate chitosan as a versatile choice for metal detoxification, as well as sequestration of organic compounds from waste/runoff waters. Chitosan and chitin are effective in the removal of herbicides[16] with good adsorption efficacy. Nevertheless, native chitosan has certain shortcomings in view of poor mechanical properties and low porosity.[20–22] A combination of chitosan and alginate in the form of assembled micro shells was utilized to detoxify 2,4-dichlorophenol and salicylic acid from hydrated medium.[23] Chitosan modified with glutaraldehyde obtained through the reaction between primary amino groups in chitosan and aldehyde moiety of glutaraldehyde enables the crosslinking and enhances the adsorption characteristics of the resultant material.[17] Chitosan could also be modified using ionic liquids,[24,25] diatomaceous earth, and silica,[26] magnetic nano particles,[27,28] and EDTA[29] to improve its chemical resistance and adsorption properties.

Recently, microwave induced preparation of activated carbon obtained from coconut shell has been reported to remove DDT with an efficacy of 84%.[30] Multiwalled carbon nanotubes (MWCNT) nano-clay and alumina are quite effective[31] to remove DDT and among these MWCNT showed a removal efficacy of 88.9%. Boussahel *et al.*[32] reported the utility of low cost carbon obtained from saw dust for DDT removal from agriculture water. The adsorption process was significantly dependent on the particle size of the adsorbent. Farmland soils rich in iron oxide was evaluated[33] to adsorb DDT and the composition of organic matter and the texture of soil had a considerable impact on the adsorption performance.

Roosen *et al.*[34] have underlined the importance of chitosan–silica hybrid materials as good adsorbents for rare-earth and transition metals in the process of valorization of bauxite residue streams. Chitosan modified with diatomaceous earth material was utilized towards the adsorption of nickel, lead, arsenic and chromium from aqueous solutions.[35–38] Diatomaceous earth is a natural siliceous material is formed from the remains of diatoms. It is an amorphous material characterized by good surface area, small particle size, adequate porosity, high permeability, and excellent adsorption capability. Nevertheless, chitosan-diatomaceous earth hybrid has not been explored in the adsorption of 4,4′-DDT from water.

Considering the above advantages, we report a new method for the adsorption of 4,4′-dichlorodiphenyltrichloroethane (4,4′-DDT) using chitosan modified with diatomaceous earth and its potential application in agricultural runoff water samples. The synthesized adsorbent was characterized comprehensively and the adsorption variables include time, pH, adsorbent dose, thermodynamics, and kinetics and elution studies. The concentration of 4,4′-DDT in aqueous solution was quantified by gas chromatography-tandem mass spectrometer (GC-MS/MS).

Materials and methods

Chemicals and reagents

Procurement of 4,4′-DDT (purity 99.5%) was done through Dr Erhenstorfer, Germany. Since, 4,4′-DDT (mol wt 354.5 g mol^{-1}) has quite low water solubility,[39] a methanolic solution was chosen as the solvent medium. Chitosan and diatomaceous earth were purchased from Sigma-Aldrich. KBr (spectroscopy grade), methanol, ethyl acetate (Merck) and other analytical grade chemicals/reagents were used as received without further purification.

Chitosan-diatomaceous earth hybrid adsorbent preparation

Chitosan-diatomaceous earth hybrid was synthesized in accordance with the previous literature with slight modifications.[35–37] Chitosan (10 g) was taken in acetic acid medium (250 mL, 1% v/v) and stirred at 300 rpm at 45 °C. To the acidic solution of chitosan in acetic acid, 15 g of diatomaceous earth was added and further stirred at same temperature for another 2 hours. After formation of white suspension, and continued agitation for a 24 h period, the solution was washed using Milli-Q water to achieve neutral pH, and air-dried for 24 hours. Under acidic conditions (pH $<pK_a$), the chitosan amine group is protonated and the protonated amine group (positively charged) could interact with negatively charged ($Si–O^-$) surface and the diatomaceous earth would deprotonate at higher pH. The resultant chitosan-diatomaceous earth hybrid[34–36] as prepared is shown in schematic illustration of the first step in Scheme 1. Additionally, to support this aspect zeta potential measurements were done and the data is presented in Fig. 1. The zeta potential measurement was conducted at specified conditions (20 mM, acetate buffer (pH 5.0) temperature at 30 °C), and the zeta potential of chitosan, diatomaceous earth and chitosan-diatomaceous earth hybrid were found to be 27.3, −19.6, and 5.9 mV respectively.[36,40] Hence, the developed chitosan–diatomaceous earth hybrid could augment the removal of 4,4′-DDT as shown in Scheme 1, step-2.[41,42] Furthermore, the surface of chitosan moiety with functional groups (NH_2 and OH), diatomaceous earth (Si–O) and the electron donor nitrogen and oxygen atoms foster interaction with electron acceptor chlorine atom (Cl) from 4,4′-DDT. Hence, the surface complexation mechanism is more facile in accordance with reported literature.[40] Further, the chitosan-diatomaceous hybrid (positively charged) could electrostatically interact with weakly acidic 4,4′-DDT (negatively charged) and this would also augment the adsorption as observed through the batch experiments and pH optimization studies.

Batch adsorption studies

A stock solution of 4,4′-DDT (1000 mg L^{-1}) in methanolic medium and working solution of 0.1 mg L^{-1} 4,4′-DDT was prepared by appropriate dilution for the adsorption process. Chitosan was mixed with diatomaceous earth at various proportions and adsorption of 4,4′-DDT pesticide was studied. Preliminary study indicated that a 40 : 60 ratio of chitosan-diatomaceous earth has good adsorption efficiency for 4,4′-DDT.

The composite of chitosan and diatomaceous earth adsorbent in the ratio 40 : 60 was characterized through various analytical and surface techniques. Zeta potential of the hybrid was acquired using a Delsa nano zeta potential analyzer (Beckman Coulter Inc., USA). Infra-red spectrum of the

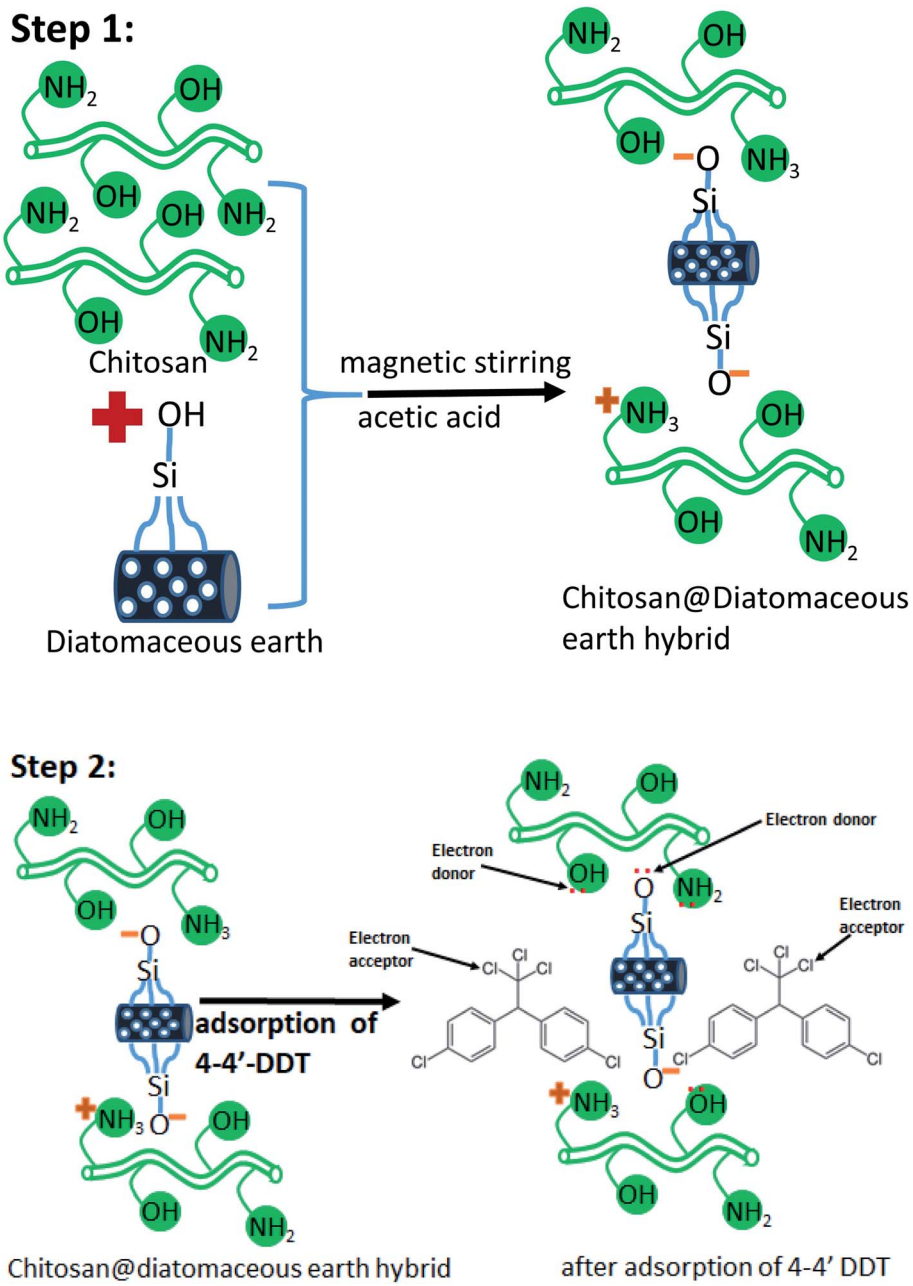

Scheme 1 Electron donor–acceptor interaction [4,4′-DDT (0.1 mg L^{-1}, pH 5.0) adsorbent amount (2.0 g L^{-1}), 60 min at 25 ± 2.0 °C].

chitosan-diatomaceous earth adsorbent was acquired by grinding approx. 2 mg with 0.1 g KBr over the wave number range 400–4000 cm^{-1} (JASCO-4200). The 4,4′-DDT concentration was measured on GC-MS/MS Shimadzu 8050 triple quadrupole mass spectrometer. Pore diameter and surface area measurements were ascertained through Brunauer–Emmett–Teller analysis (Quantachrome instrument, NovaWin software). FESEM (Carl Zeiss Supra 55) and an EDX analysis (Ametek) was used to comprehend the surface attributes and elemental composition. PANalytical Epsilon 1 XRF spectrometer was utilized for verification of distinct Cl peaks and a Metrohm 867 pH meter was employed to control the pH of the reaction medium. Thermal degradation of chitosan-diatomaceous earth was performed in N_2 atmosphere (Shimadzu DTA 60 differential thermal analyzer) in the range 35–800 °C. X-ray diffraction study of the hybrid adsorbent was done with Rigaku Ultima IV X-ray diffractometer (Cu-Kα, 1.54 Å). The XPS spectrum for the characteristic peaks of Si, Cl was acquired using a Thermo Fischer XPS model instrument. The UV spectrum (Shimadzu UV-1800) of 4,4′-DDT was done using 10 mm path length quartz cells over 200–400 nm wavelength range.

Adsorption and analysis of 4,4′-DDT

A fixed amount of chitosan-diatomaceous earth adsorbent (0.2 g) was transferred to a Erlenmeyer flask containing 100 millilitres of

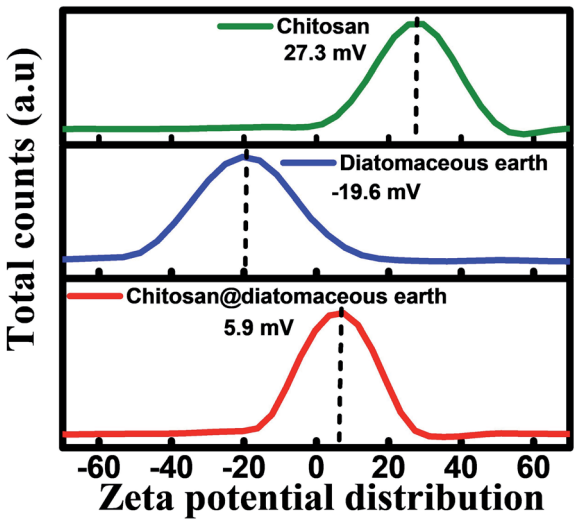

Fig. 1 Zeta potentials distribution of [(chitosan, dark green line), (diatomaceous earth, dark blue line) and (chitosan@diatomaceous earth hybrid, red line)], were incubated with acetate buffer (500 μL, 20 mM; pH 5.0) and temperature 30 °C.

4,4′-DDT solution (100 μg L^{-1}, pH 5.0) and equilibrated (magnetic stirring) for 1 h duration. The equilibrium adsorption capacity (q_e) of the hybrid adsorbent was calculated as

$$q_e = \frac{(C_o - C_e)v}{w} \quad (1)$$

v and w are the volume of 4,4′-DDT in aqueous phase in litre and weight of chitosan-diatomaceous earth adsorbent in gram.

In every analysis, after adsorption, the solution was filtered, the adsorbent was dried, 4,4′-DDT was eluted from adsorbent with ethyl acetate, and taken in a 2 mL volume GC vial and 1 μL was injected into GC-MS/MS system to quantify the 4,4′-DDT concentration. For GC-MS/MS measurements, a five-point calibration curve was acquired from standards in 0.01, 0.02, 0.05, 0.10, 0.2 mg L^{-1} (Fig S1(a)).† The mobile phase was ultra-pure helium gas, collision gas was ultrapure Argon. The flow rate of 1.0 mL min^{-1} was maintained on GC column HP-5MS Ultra inert 30 m length, 0.25 mm internal diameter, 0.25 μm film thickness. Linear velocity mode was used for flow control. Injector port temperature was maintained at 300 °C. A purge flow of 3 mL min^{-1} was used. Split ratio maintained at 1 : 20. The initial oven temperature was fixed at 60 °C for 5 min, with a gradual increase to 170 °C @ 40 °C min^{-1}, then further to 310 °C @ 10 °C min^{-1}, and final temp of 310 °C was maintained for 3 min. The total runtime is 20.75 min. Transfer line temp was maintained at 300 °C. Electron impact ionization was used @ 70 eV to ionize 4,4′-DDT. MRM acquisition mode was used. 235 m/z was selected in Quadrupole-1 from the EI source fragment, and further fragmented in Quadrupole-2 using hi-pure argon gas, and from fragments of 165 m/z and 199 m/z, the more abundant and stable ion 165 m/z was selected for Quadrupole-3. Detector gain was maintained at +0.3 kV. EI source Fragmented ion (m/z 235) was perceived as the precursor for 4,4′-DDT. The fragmentation was done in mass spectrometer with argon as collision gas resulting in the observation of distinct peaks characteristic of the product ions (m/z 165 and 199) respectively (Fig S1(b) and (c)†). Response was good for the product ion (m/z 165) and seemed quite appropriate to describe the fragmentation and quantitation. Calibration data points were obtained by varying the concentrations of 4,4′-DDT (0.01–0.2 mg L^{-1}) The sample concentrations were ascertained through peak area and the blank and 4,4′-DDT peaks (Fig S1(d)†) and peak area quantified the concentration of 4,4′-DDT.

Results and discussion

Surface features of the chitosan-diatomaceous earth adsorbent

Morphological features of the glucosamine polysaccharide-diatomaceous earth surface before and after adsorption of 4,4′-DDT was visualized through scanning electron microscopy (Fig. 2). The magnified images showed that the adsorbent has a relatively coarse morphology with micro and mesopores to enable the adsorption of 4,4′-DDT on the adsorbent surface. SEM image of adsorbent after adsorption with 4,4′-DDT has a comparatively smoother surface texture. Moreover, the uneven cavities are covered, and this could be ascribed to the presence of 4,4′-DDT onto chitosan-diatomaceous earth hybrid surface. The surface composition from energy dispersive X-ray spectroscopy (EDX) indicated C, N, O, Si and Cl (Fig. 2(d)) as elemental peaks. The appearance of chlorine peak confirms the presence of 4,4′-DDT on the chitosan-diatomaceous earth hybrid surface.

The BET isotherm (Fig. 3) plot from the adsorption and desorption curve resulted in the surface area of hybrid adsorbent as 1.589 m^2 g^{-1}. The average pore volume and pore diameter of the biopolymer–silica based material were 0.004 cm^3 g^{-1} and 2.164 nm analogous to microporous nature. It shows that chitosan blocked several pores in diatomaceous earth. Adsorption is favoured by the interaction between 4,4′-DDT and surface functionalities on the chitosan-diatomaceous earth hybrid adsorbent.

X-ray fluorescence spectrometry was employed to validate the adsorption of 4,4′-DDT onto the hybrid adsorbent surface. The spectrum was recorded for chitosan-diatomaceous earth hybrid before and after adsorption of 4,4′-DDT. Fig. 4 shows the overlapped XRF spectra for chitosan-diatomaceous earth hybrid sorbent prior to and after the adsorption of 4,4′-DDT. An intense peak after adsorption at 2.62 keV is characteristic of chlorine in 4,4′-DDT indicating the effective adsorption of 4,4′-DDT onto the sorbent chitosan-diatomaceous earth hybrid. A small and weak intensity peak at the same energy before adsorption could be attributed to residual chlorine in the water. The FT-IR study was valuable in the identification of functional groups of 4,4′-DDT on chitosan-diatomaceous earth hybrid (Fig. 5). The FT-IR spectrum of chitosan-diatomaceous earth hybrid before adsorption has well defined peaks at 1089 cm^{-1} which is indicative of the C–O skeletal vibrations and at 3116–3268 cm^{-1} reflecting the N–H and O–H stretching band vibrations.[43] As obvious 2883 cm^{-1} is a characteristic trait of C–H stretching vibration. Vibrations at 1660 cm^{-1} corresponds to C=O

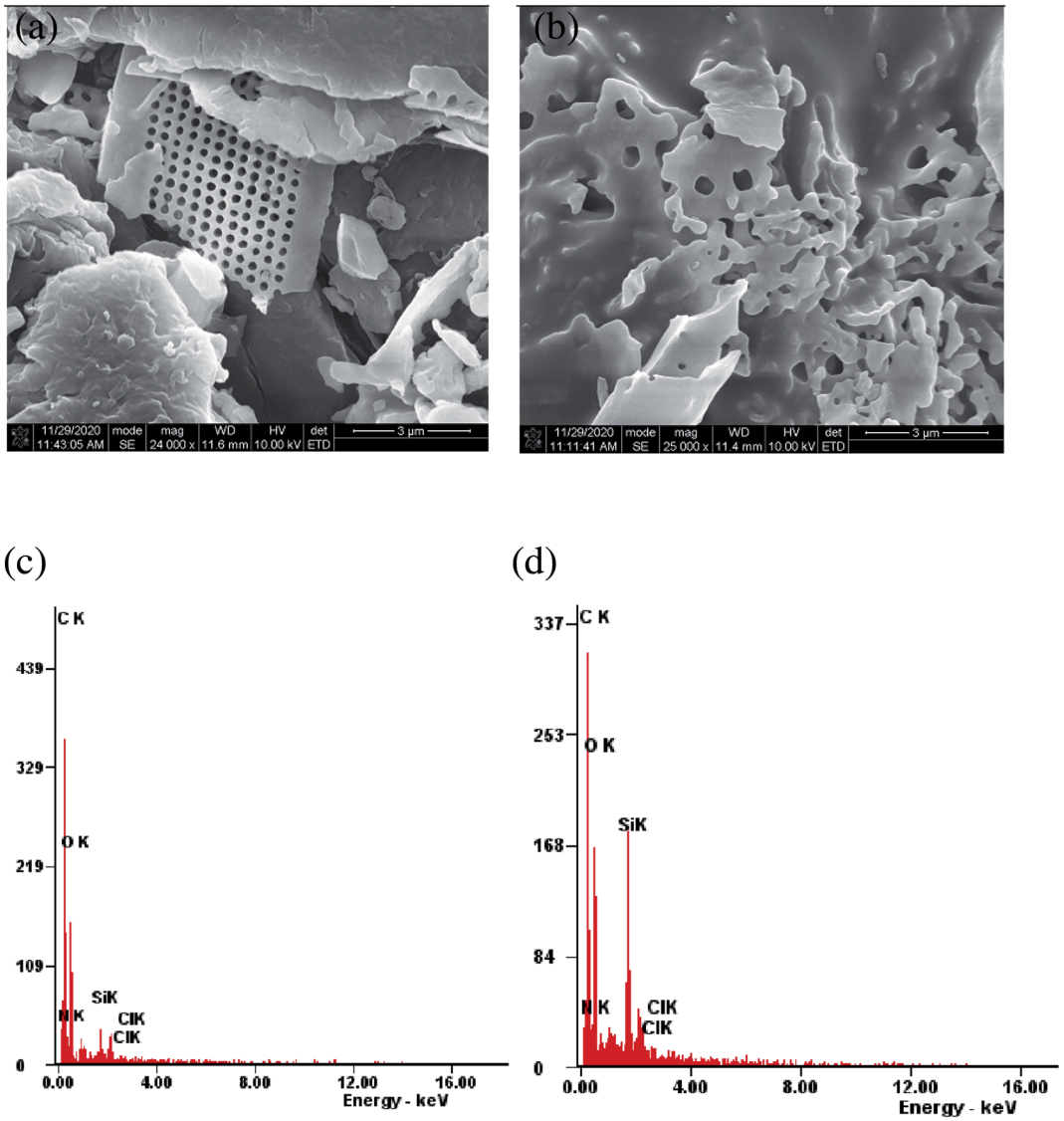

Fig. 2 SEM images of hybrid adsorbent (a) before and (b) after adsorption of 4,4′-DDT, energy dispersive X-ray spectrum (EDX) (c) before adsorption; (d) after adsorption of 4,4′-DDT concentration (0.1 mg L^{-1}, pH 5.0) adsorbent amount (2.0 g L^{-1}), 60 min at 25 ± 2.0 °C.

stretching of amide bond. The Si–O and Si–O–Si groups[43,44] and the deformations are observed around 620 cm^{-1}. The FTIR-spectra after adsorption of 4,4′-DDT showed a definite shift in N–H vibrational frequency to 3268 cm^{-1} indicating that the amine groups are indeed involved in the interaction mechanism.

The thermogravimetric analysis (TGA) (Fig S2†) study revealed the thermal stability of the chitosan-diatomaceous earth hybrid. The first step in the range 70–250 °C is ascribed to water evaporation from the adsorbent, the second step pyrolysis with 40% weight reduction from 250 to 350 °C corresponding to the heterolytic depolymerization and the final stage between 360 and 750 °C relates to the decomposition of chitosan and complete loss of carbon and remaining 55–60% mass corresponds to silica.[45] The UV analytical data was acquired before and after 4,4′-DDT adsorption onto the hybrid adsorbent. Prior to adsorption, the solution showed a UV Max at 248 nm and 338 nm, which corresponds to 4,4′-DDT. The resulting solution after 4,4′-DDT adsorption was subjected to UV analysis which showed a markedly low absorbance in the solution phase and this indicates 4,4′-DDT adsorption is effectively adsorbed on the chitosan-diatomaceous earth hybrid surface (Fig S3†). Powder XRD studies was carried out in order to ascertain the amorphous or crystalline nature of chitosan-diatomaceous earth hybrid before and after the adsorption of 4,4′-DDT, as displayed in Fig S4.† The XRD profiles had no discernible changes and the sharp diffraction pattern is characteristic of more crystalline nature in this glucosamine–silica hybrid material. The broad peak around $2\theta = 22°$ is the (002) diffraction pattern of chitosan and peaks at 26.73°, 36° and 31° correspond to the quartz and crystoballite forms of silica.[46] More degree of crystallites in an amorphous matrix is observable in the biopolymer-diatomaceous earth surface. Survey scan X-ray photoelectron spectroscopy (XPS) analysis revealed

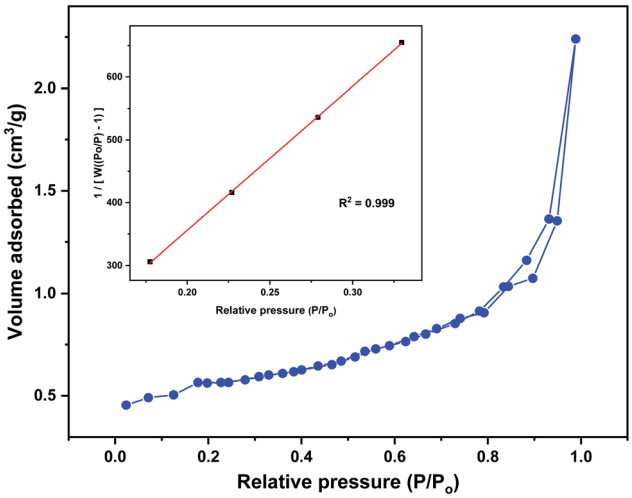

Fig. 3 BET isotherm plot of chitosan-diatomaceous earth hybrid.

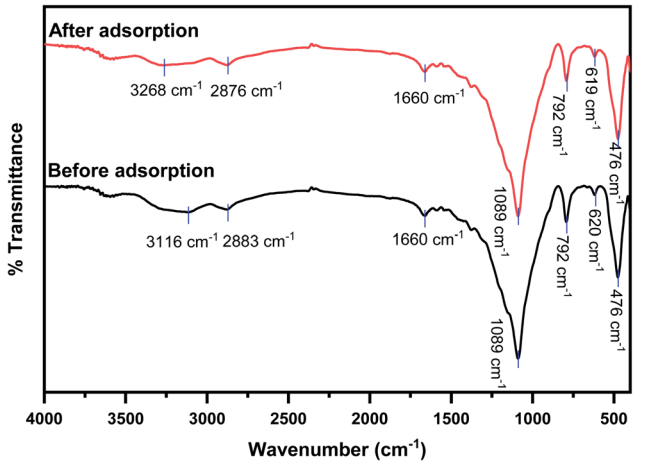

Fig. 5 Infra-red spectrum of hybrid adsorbent [4,4′-DDT (0.1 mg L^{-1}, pH 5.0); adsorbent amount (2.0 g L^{-1}), 60 min equilibration at 25 ± 2.0 °C].

carbon, silicon, nitrogen and oxygen on the chitosan-diatomaceous earth surface as shown in Fig. 6(a). The identifiable peaks at 102, 285, 401, and 531.5 eV can be ascribed to Si2p (Fig. 6(b)), C1s (Fig. 6(c)), O1s (Fig. 6(d)), and N1s (Fig. 6(e)). The C1s spectrum dual peaks deconvoluted into 284.7 eV, 286.5 eV Fig. 6(c) represent C–C and C–O from chitosan.[47] Likewise, the N1s spectrum can be separated as 398, and 401.2 eV, attributed to amine –NH_2 group[37] as shown in Fig. 6(e). In addition to silicon, carbon, nitrogen, oxygen from chitosan-diatomaceous earth hybrid, adsorption of 4,4′-DDT onto the hybrid adsorbent shows Cl peaks and these facts support that 4,4′-DDT is adsorbed quite well onto the porous diatomaceous earth hybrid surface and as shown in Fig. 6(f) binding energy in Cl2p spectra above 200 eV indicates organic chlorine C–Cl bond.[47]

Analytical parameters and validation

The analytical method in accordance with SANTE/12682/2019 was used in the estimation of 4,4′-DDT on GC-MS/MS.[48] There was no distinct interference reiterating that the method has adequate selectivity in the analysis of 4,4′-DDT. With calibration standards prepared over the range 0.01–0.2 mg L^{-1}, a well-defined linearity with a high regression coefficient value of 0.99 was attained and the precision was checked by spiking six replicates of 0.01 mg L^{-1} 4,4′-DDT and injected in GC-MS/MS along with other standard calibration solutions. With a precision of 3.7%, the limit of detection (ICH guidelines) for the developed method was 0.001 mg L^{-1} and the limit of quantification for the method was 0.003 mg L^{-1}.

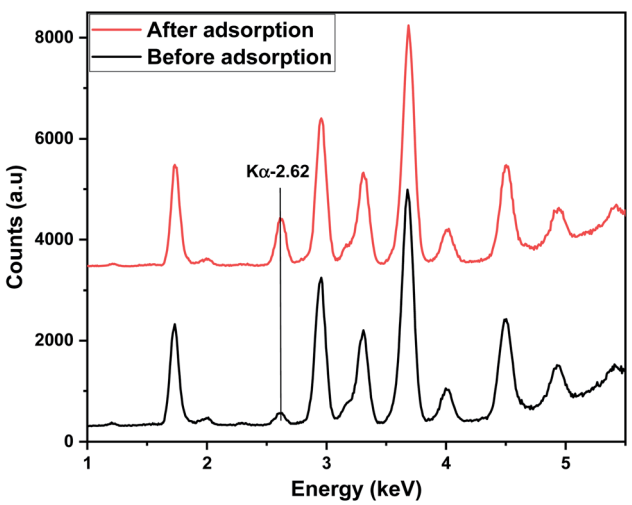

Fig. 4 XRF spectra of hybrid adsorbent [4,4′-DDT (0.1 mg L^{-1}, pH 5.0) adsorbent amount (2.0 g L^{-1}), 60 min at 25 °C].

Effect of pH and amount of chitosan-diatomaceous earth hybrid

The adsorption of 4,4′-DDT on chitosan-diatomaceous earth hybrid at various initial pH levels including 3, 5, 7, 9, 11 were studied and is depicted in Fig. 7(a). The studies indicate that the adsorption is augmented with rise in pH and attained its peak at pH 5.0. At pH 5.0, 99% adsorption was achieved and, 14.78% adsorption at pH 3.0 while 46.4% adsorption of 4,4′-DDT was observed at pH 9.0 weakly acidic to neutral pH favours adsorption of 4,4′-DDT on the hybrid adsorbent surface. This can be explained due to the amine groups (-NH_2) in chitosan and diatomaceous earth hybrid (silica-OH) are mainly responsible for adsorption. At lower pH below 5, –NH_2 could exist as protonated NH_3^+ in an acidic environment which lowers the adsorption. The extent of amine group protonation is diminished at high pH values and with increase in pH the decrease in adsorption percentage is ascribed to the fact that the hybrid adsorbent surface has a reduced positive charge on its surface. As mentioned before in the adsorbent preparation procedure, and in Scheme 1 the electrostatic interaction between $NH_3^+\cdots SiO^-$ and electron donor Cl groups in 4,4′-DDT favours the adsorption. As Cl is also an electron withdrawing group, it enables the adjacent proton to be acidic, thereby enabling effective interaction with chitosan-diatomaceous earth in weakly acidic medium. Adsorbent dosage is quite important

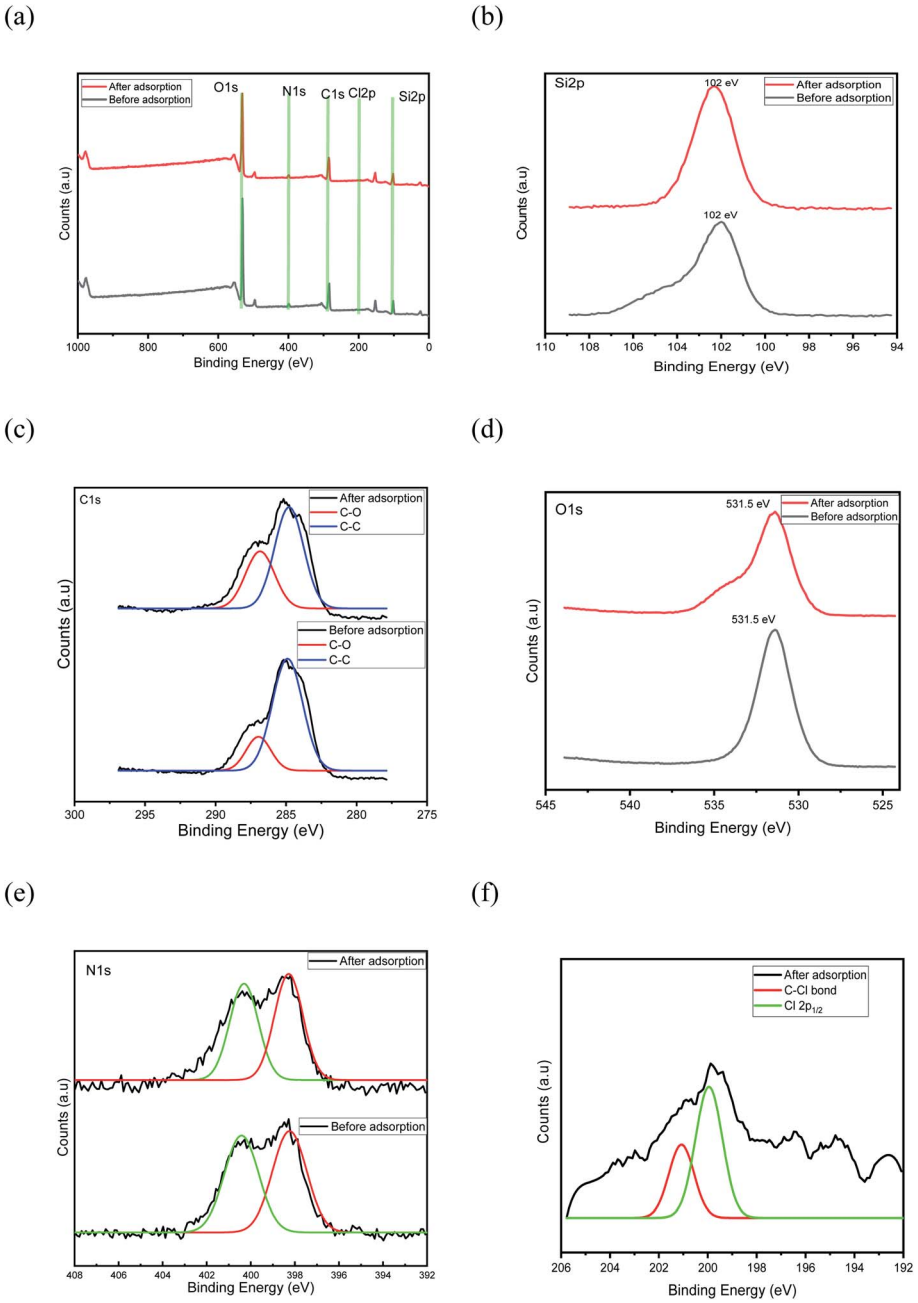

Fig. 6 XPS of hybrid adsorbent (a) survey scan, (b) Si2p spectra, (c) C1s spectra, (d) O1s spectra, (e) N1s spectra and (f) Cl2p spectra [4,4′-DDT (0.1 mg L^{-1}, pH 5.0); adsorbent amount (2.0 g L^{-1}), 60 min equilibration at 25 ± 2.0 °C].

parameter as it serves as an indicator to quantify the adsorption capacity for a specified concentration of 4,4′-DDT. Fig. 7(b) depicts the variation of chitosan-diatomaceous earth hybrid amount and the percentage adsorption of 4,4′-DDT increased with the rise in adsorbent amount and this feature can be traced to the availability of active adsorption sites on the glucosamine polysaccharide-diatomaceous earth surface.

Adsorption isotherms and thermodynamics

The transfer of 4,4′-DDT from solution phase on to the chitosan-diatomaceous earth hybrid at equilibrium and at constant temperature can be best described through the classic Langmuir isotherm (linear) equation[51]

$$\frac{C_e}{q_e} = \frac{1}{q_{max}} C_e + \frac{1}{q_{max} b} \quad (2)$$

where q_e (mg g^{-1}) and C_e (mg L^{-1}) are the equilibrium adsorption capacity and the equilibrium concentration of 4,4′-DDT in solution respectively. q_{max} is referred as Langmuir adsorption capacity per unit mass of hybrid adsorbent and b (L mg^{-1}) is Langmuir constant. The Langmuir constant is linked to a dimensionless constant ($R_L = 1/(1 + bC_o)$) and the R_L value between 0–1 justifies the adsorption.

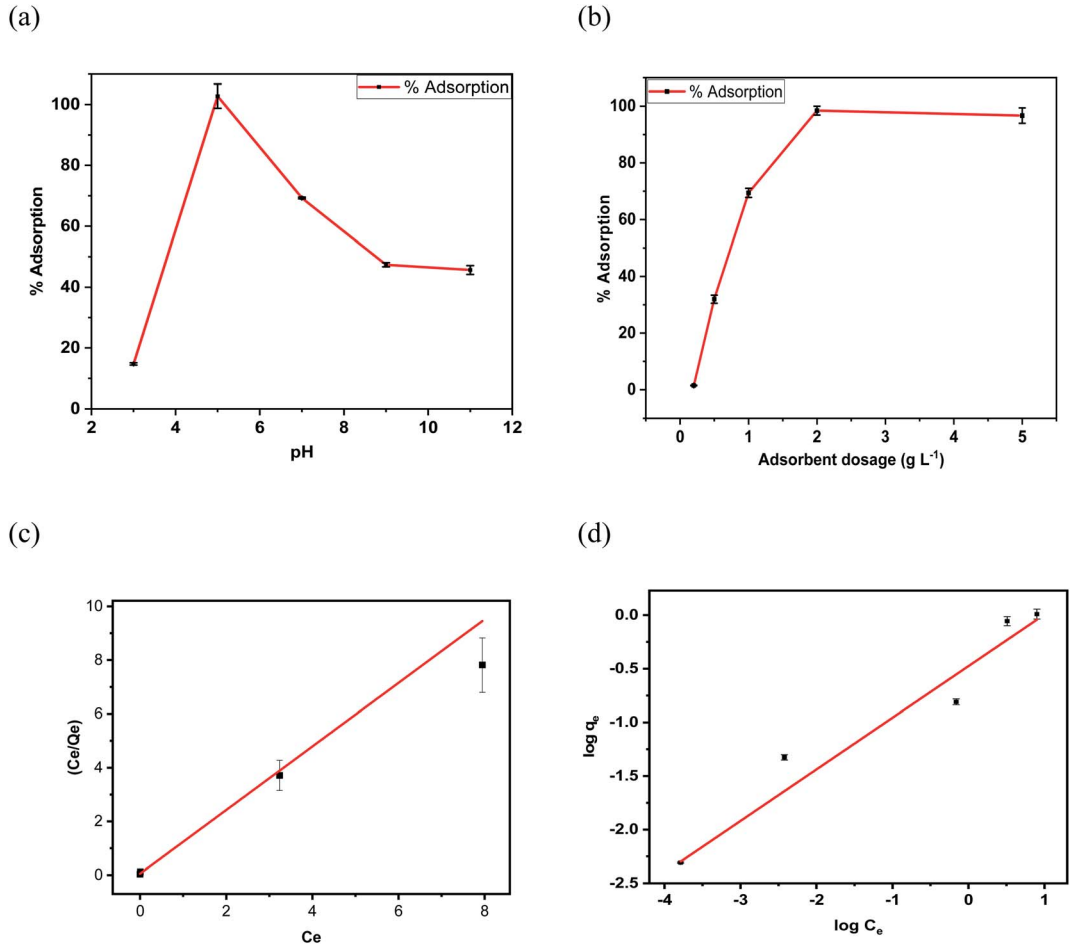

Fig. 7 (a) Variation of pH, (b) variation of hybrid adsorbent amount (c) Linear Langmuir isotherm plot, (d) Freundlich model [A working solution of 4,4′-DDT concentration 0.1 mg L^{-1}, pH 5.0 at adsorbent amount (2.0 g L^{-1}), 60 min equilibration at 25 ± 2.0 °C], (a) pH 3.0, 5.0,7.0,9.0 and 11.0 (b) 0.05–5.0 g L^{-1} (c and d) 0.01, 0.1, 1, 5 and 10 mg L^{-1}.

The Freundlich model (linear) determines the affinity between 4,4′-DDT and chitosan-diatomaceous earth hybrid surface.

$$\log (q_e) = \log (K_F) + \frac{1}{n}\log C_e \quad (3)$$

From the linearity in the relation between the parameters log q_e against log C_e the K_F and n values were obtained. Fig. 7(c and d) represent the graphical relation involving C_e/q_e *versus* equilibrium concentration (C_e) of 4,4′-DDT in aqueous medium and logarithmic relation (log q_e) against the equilibrium concentration (log C_e) of 4,4′-DDT Langmuir and Freundlich adsorption isotherm parameters[51] experimentally obtained from the adsorption study are given in Table 1. The Langmuir adsorption capacity was found to be 968 μg g^{-1} and is more in favour of the Langmuir adsorption model having ($R^2 = 0.987$) in comparison with Freundlich isotherm ($R^2 = 0.959$).

Adsorption of 4,4′-DDT is more facile closer to room temperature and the results indicated that at 30 °C, 94% of DDT was adsorbed in comparison to 30% at an elevated temperature of 60 °C. With rise in temperature the affinity between DDT and hybrid adsorbent become weaker resulting in desorption thereby lessening the adsorption capacity of chitosan-diatomaceous earth hybrid. The adsorption phenomenon between 4,4′-DDT and chitosan-diatomaceous earth hybrid is primarily more of physical adsorption. Thermodynamic parameters namely, enthalpy, entropy and free energy highlight the effect of temperature on the adsorption of DDT on the biopolymer–silica surface. Imposing thermodynamic equilibrium conditions, the reaction Gibbs energy, $\Delta G_r = 0$ and $\Delta G_r o = -RT \ln K_{eq}$. The K_{eq} is defined as the ratio of $[DDT]_{adsorbent}$

Table 1 Experimental isotherm parameters derived from two isotherm models

	q_o (mg g^{-1})	b (L mg^{-1})	R_L	R^2
Langmuir	0.968	0.043	0.295	0.987
Freundlich	K_F ($mg^{1-1/n}$ g^{-1} $L^{1/n}$)	n	—	R^2
	0.3388	2.0781	—	0.959

$_{surface}/[DDT]_{solution}$ at varying temperature. The thermodynamics is described through the Van't Hoff equation[52] that yields the other associated variables from the graphical correlation of ln K against $1/T$ (Fig. 8).

$$\ln K_{eq} = -\frac{\Delta H^{o}}{R}\left(\frac{1}{T}\right) + \frac{\Delta S^{o}}{R} \quad (4)$$

The adsorption process for 4,4′-DDT is spontaneous as obvious from the negative free energy change with reduced randomness (-136.098 J mol^{-1} K^{-1}) on the glucosamine polysaccharide–silica adsorbent surface. The exothermicity (-42.885 kJ mol^{-1}) with an appreciably more negative entropy (Table 2) enables that the adsorption of 4,4′-DDT is spontaneous.[41]

Kinetic aspects influencing adsorption of 4,4′-DDT

Kinetics of adsorption of 4,4′-DDT was studied at equilibration intervals of 1, 5, 15, 30 and 60 min, the amount of 4,4′-DDT adsorbed on to chitosan-diatomaceous earth was calculated. The concentration of 4,4′-DDT after the attainment of equilibrium was plotted against varying time duration. Fig. 9 shows the adsorption profile of 4,4′-DDT at different time intervals for the respective kinetic models. At equilibrium, the 4,4′-DDT molecules in the solution are in a state of dynamic equilibrium with the hybrid adsorbent surface. The kinetics of 4,4′-DDT uptake from the hybrid adsorbent surface was established with the aid of pseudo first and second-order kinetic models[51] described as

$$\log (q_e - q_t) = \log q_e - \frac{k_1}{2.303} t \quad (5)$$

$$\frac{t}{q_t} = \frac{1}{k_2 q_e^{2}} + \frac{t}{q_e} \quad (6)$$

$$q_t = k_i t^{1/2} + C \quad (7)$$

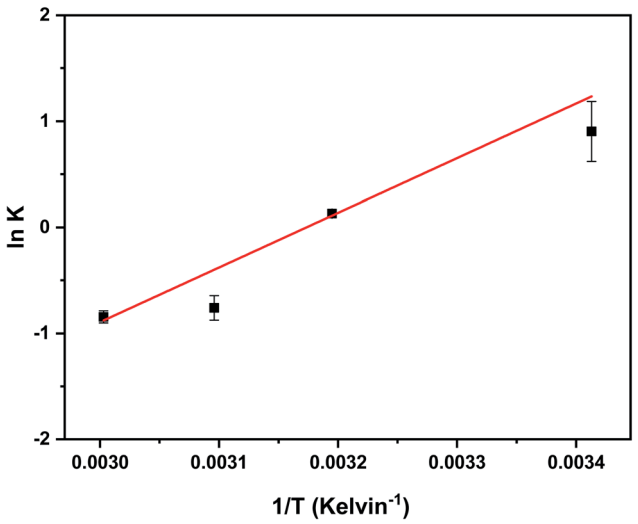

Fig. 8 The Van't Hoff representation of ln K against inverse of temperature between temperatures range 20–60 °C.

Table 2 Thermodynamics of 4,4′-DDT adsorption on the hybrid adsorbent surface

Temperature (K)	ΔG^{0} (kJ mol^{-1})	ΔS^{o} (J mol^{-1} K^{-1})	ΔH^{o} (kJ mol^{-1})
293	−2.203	−136.098	−42.885
303	−7.405		
313	−0.339		
323	2.045		
333	2.344		

The first-order kinetic model is generally applicable at low concentration range of 4,4′-DDT and the second-order kinetic model recognizes the step involving rate control as an exchange reaction. The regression coefficient as obtained through the pseudo-second-order model was 0.999 and this affirmed that 4,4′-DDT adsorption on the chitosan-diatomaceous earth hybrid surface is most appropriately defined through the pseudo second order kinetics (Table 3). Adsorption on to the polysaccharide–silica surface, diffusion into the pores of the hybrid adsorbent, and boundary layer influence the transfer of 4,4′-DDT from the solution phase onto the chitosan-diatomaceous earth hybrid solid material. The Weber–Morris intra-particle diffusion (eqn (7)) illustrates that 4,4′-DDT adsorption onto the chitosan-diatomaceous earth hybrid could also be attributed to the boundary layer feature as well.

Regeneration of adsorbent

The regeneration potential of the hybrid adsorbent was checked using ethyl acetate and dichloromethane as solvents for desorption of 4,4′ DDT. Although, both solvents showed good ability to desorb 4,4′-DDT, ethyl acetate was preferred owing to the toxicity of dichloromethane. The surface of the chitosan–silica surface was conditioned by water wash prior to desorption for successive cycles. For a period of three adsorption–desorption cycles (Table S1†) an efficacy of 97%, 95%, and 91% was realized. The resultant solution after desorption with the ester was subjected mass spectrum characterization with GC-MS/MS in electron impact ionization mode. A precursor ion with m/z 235 was obtained indicating the fragmentation of 4,4′-DDT after EI ionization (Fig S5†) which matches with fragmentation pattern of 4,4′-DDT (Fig S6†). This result confirmed the effectiveness of 4,4′-DDT adsorption onto the chitosan-diatomaceous earth hybrid.[49,50]

Impact of other pesticides and proof of concept in farm water sample

The impact of certain pesticides that have a bearing in structure to 4,4′-DDT on the adsorption of 4,4′-DDT onto chitosan-diatomaceous earth was studied through spike recovery of 0.1 mg L^{-1} concentration of alpha-HCH, beta-HCH, gamma-HCH, Endosulfan-I, Endosulfan-II. The data presented in Table S2† with an adsorption efficiency of >95% shows that the structurally similar pesticides do not significantly lower the

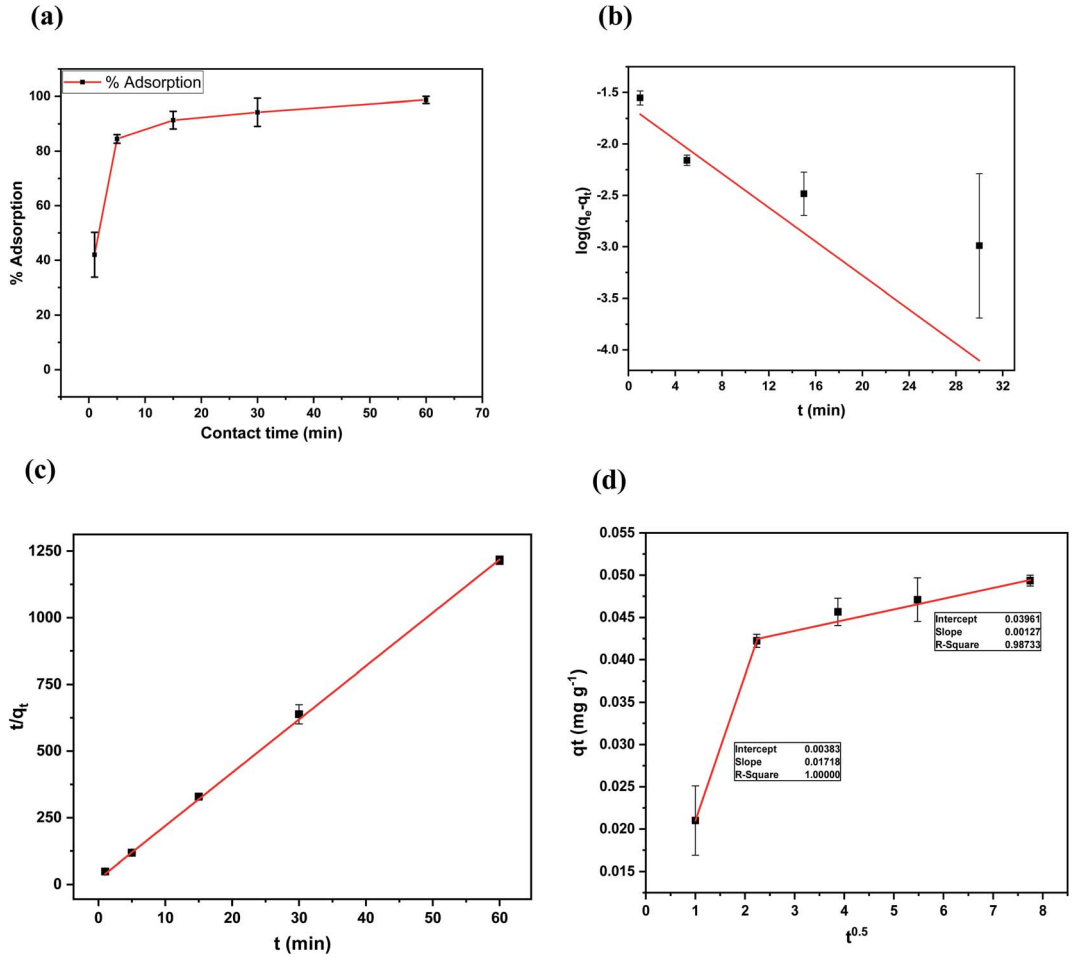

Fig. 9 (a) Kinetics of adsorption of 4,4′-DDT showing variation of equilibration time for the kinetic models pseudo-first, second order (b and c) and Weber–Morris intra-particle diffusion (d) [4,4′-DDT (0.1 mg L^{-1}, pH 5.0 adsorbent amount 2.0 g L^{-1}), temperature 25 ± 2.0 °C].

Table 3 Kinetic data for 4,4′-DDT adsorption on chitosan-diatomaceous earth hybrid surface

C_o (mg L^{-1})	q_e (mg g^{-1})	k_2 (g mg^{-1} min^{-1})	R_2^2	k_1 (min^{-1})	R_1^2	k_{int} (mg g^{-1} $min^{-0.5}$)
0.1	0.050	3.7318	0.9994	0.190228	0.587	0.00127

adsorption of 4,4′-DDT and adsorption of 4,4′-DDT under the experimental conditions.

Additionally, the adsorption capacity of chitosan-diatomaceous earth hybrid for 4,4′-DDT was also tested on water collected from a local agriculture farm. The farm water characteristics and the location coordinates have been reported previously by our group in an earlier study.[53] Approximately, a 25 L volume of water was sampled from an agricultural field having a total hardness of over 1000 ppm and a near neutral pH. The pesticide 4,4′-DDT was not present as such in the sample and hence the adsorption experiments was done by spiking 4,4′-DDT at different concentrations and was found that 90% (Table S3†) of 4,4′-DDT was adsorbed onto this hybrid adsorbent surface. This proof of concept indicates that chitosan-diatomaceous earth hybrid has the potential to adsorb 4,4′-DDT pesticide from field water.

Conclusions

This work has underlined the effective extraction of a persistent organic pollutant and toxic pesticide, 4,4′-DDT from water using chitosan-diatomaceous earth hybrid as an adsorbent. Adsorption was facile in slightly acidic reaction conditions in 1 h duration having a Langmuir adsorption capacity of 968 μg g^{-1} and pseudo-second-order kinetics was favoured with a regression coefficient of 0.99. The stability of the adsorbent was evident under the experimental conditions and the thermodynamic data ensured the spontaneity (negative free energy) exothermicity (negative enthalpy) and decreased randomness (negative entropy) at the glucosamine polysaccharide-diatomaceous earth surface. Diverse surface characterization and zeta potential measurements supported the mechanism with the involvement of the functional and the donor Cl groups

in the interaction. Reuse of the adsorbent using ethyl acetate for three cycles and recovery (>91%) of 4,4′-DDT was effective in the presence of other pesticides such as alpha-HCH, beta-HCH, gamma-HCH, Endosulfan-I, and Endosulfan-II. Fragmentation data from mass spectrum confirmed the successful regeneration with ethyl acetate through the obtained product ions. The hybrid adsorbent could remove above 90% DDT from farm water. Indeed, tapping the potential of this glucosamine based biopolymer along with diatomaceous earth hybrid adsorbent material paves the path toward blending more such sustainable materials for environmental remediation.

Conflicts of interest

There are no conflicts to declare.

Acknowledgements

Thanks to the Central Analytical Laboratory, BITS Pilani, Hyderabad Campus for providing technical support. Vimta Labs Ltd, Hyderabad, India is also acknowledged for extending support toward GC-MS/MS analysis and other experiments in their sophisticated instrumentation laboratory. Thanks to Sprint testing solutions, Mumbai, India, for support in performing few surface characterizations.

References

1 U.S. EPA, *DDT - A Brief History and Status*, available from: https://www.epa.gov/ingredients-used-pesticide-products/ddt-brief-history-and-status.
2 World Health Organization, *DDT and its derivatives*, Environmental Health Criteria., Geneva, Switzerland, 1979, vol. 9.
3 World Health Organization, Environmental aspects, *DDT and its derivatives*, Environmental Health Criteria, Geneva, Switzerland, 1989, vol. 83.
4 M. S. El-Shahawi and A. Hamza, *Talanta*, 2010, **80**, 1587–1597.
5 H. C. Agarwal, D. K. Singh and V. B. Sharma, *J. Environ. Sci. Health B*, 1994, **29**, 73–86.
6 M. F. Zaranyika, E. Matimati and P. Mushonga, *S. Afr.*, 2020, **9**, e00467.
7 J. L. Gerberding, *Toxicology Profile for: 4,4'-DDT, 4,4'-DDE, 4,4'-DDD*, U. S. Department of Human Health & Human Services, Agency for Toxic Substances and Disease Registry, 2002, vol. 16.
8 The Hazardous Substances Data Bank (HSDB). https://pubchem.ncbi.nlm.nih.gov/source/hsdb/200 (Accessed Feb 2022).
9 I. Ali, *Chem. Rev.*, 2012, **112**, 5073–5091.
10 B. Srivastava, V. Jhelum, D. D. Basu and P. K. Patanjali, *J. Sci. Ind. Res.*, 2009, **68**, 839–850.
11 J. Kaushal, M. Khatri and S. K. Arya, *Ecotoxicol. Environ. Saf.*, 2021, **207**, 111483.
12 I. A. Saleh, N. Zouari and A. A. Mohammad, *Environ. Technol. Innovation*, 2020, **19**, 101026.
13 *WHO Guidelines for Drinking-water Quality*, ed. M. Sheffer, 4th edn, 2011, p. 349.
14 Indian standard: Drinking water -Specification IS 10500-2012, amended in 2021.
15 J. O. Ighalo, A. G. Adenivi and A. A. Adelodun, *J. Ind. Eng. Chem.*, 2021, **93**, 117–137.
16 H. El Harmoudi, L. El Gaini, E. Daoudi, M. Rhazi, Y. Boughaleb, M. A. El Mhammedi, A. Migalska-Zalas and M. Bakasse, *Opt. Mater.*, 2014, **36**, 1471–1477.
17 O. A. C. Monteiro Jr and C. Airoldi, *Int. J. Biol. Macromol.*, 1999, **26**, 119–128.
18 R. Venkatachalapathy and A. S. B. Packirisamy, *Process Biochem.*, 2020, **94**, 305–312.
19 A. Bhatnagar and M. Sillanpaa, *Adv. Colloid Interface Sci.*, 2009, **152**, 26–38.
20 H. Karimi and M. AliAyati, *J. Cleaner Prod.*, 2021, **291**, 125880.
21 P. Pal, A. Pal, K. Nakashima and B. K. Yadav, *Chemosphere*, 2021, **266**, 128934.
22 P. S. Bakshi, D. S. Kumar, K. Kadirvelu and N. S. Kumar, *Int. J. Biol. Macromol.*, 2020, **150**, 1072–1083.
23 Y. Ding, Y. Zhao, X. Tao, Y. Z. Zheng and J. F. Chen, *Polymer.*, 2009, **50**, 2841–2846.
24 T. Mitra, G. Sailakshmi, A. Gnanamani and A. B. Mandal, *J. Mater. Sci.: Mater. Med.*, 2012, **23**, 1309–1321.
25 F. Naseeruteen and N. S. AbdulHamid, *Int. J. Biol. Macromol.*, 2018, **107**, 1270–1277.
26 T. M. Budnyak, I. V. Pylypchuk, V. A. Tertykh, E. S. Yanovska and D. Kolodynska, *Nanoscale Res. Lett.*, 2015, **10**, 87.
27 D. Wu, L. Zhang, L. Wang, B. Zhu and L. Fan, *J. Chem. Technol. Biotechnol.*, 2011, **86**, 345–352.
28 D. Malwal and P. Gopinath, *Colloids Interface Sci. Commun.*, 2017, **19**, 14–19.
29 E. Repo, J. Warcho, A. Bhatnagar and M. Sillanpää, *J. Colloid Interface Sci.*, 2011, **358**, 261–267.
30 A. Aziz, M. N. N. Khan, M. F. M. Yusop, E. M. J. Jaya, M. A. T. Jaya and M. A. Ahmad, *Int. J. Chem. Eng.*, 2021, **2021**, 9331386.
31 M. R. Taha and S. Mobasser, *PLoS One*, 2015, **10**, e0144071.
32 R. Boussahel, H. Irinislimane, D. Harik and K. M. Moussaoui, *Chem. Eng. Commun.*, 2009, **196**, 1547–1558.
33 D. Cheng, J. Yu, T. Wang, W. Chen and P. Guo, *Pol. J. Environ. Stud.*, 2014, **23**, 1527–1535.
34 J. Roosen, J. Spooren and K. Binnemans, *J. Mater. Chem. A*, 2014, **2**, 19415–19426.
35 S. S. Salih and T. K. Ghosh, *J. Environ. Chem. Eng.*, 2018, **6**, 435–443.
36 S. S. Salih and T. K. Ghosh, *Int. J. Biol. Macromol.*, 2018, **106**, 602–610.
37 S. S. Salih, A. Mahdi, M. Kadhom and T. K. Ghosh, *J. Environ. Chem. Eng.*, 2019, **7**, 103407.
38 S. S. Salih and T. K. Ghosh, *Environ. Processes*, 2017, **5**, 23–29.
39 P. N. Breysse, *Toxicological Profile: for DDT, DDE, and DDE, Agency for Toxic Substances and Disease Registry*, U.S. Department of Health and Human Services, December 2019.

40 M. R. Taha and S. Mobasser, *PLoS One*, 2015, **10**(12), e0144071.
41 X. Cao, H. Han, G. Yang, X. Gong and J. Jing, *Mar. Pollut. Bull.*, 2011, **62**(11), 2370–2376.
42 R. Boussahel, H. Irinislimane, D. Harik and K. M. Moussaoui, *Chem. Eng. Commun.*, 2009, **196**(12), 1547–1558.
43 B. Galzerano, C. I. Cabello and B. Liguori, *Materials*, 2020, **13**(17), 3760.
44 R. Tian, O. Seitz and J. Gao, *Langmuir*, 2010, **26**(7), 4563–4566.
45 S. S. Salih and T. K. Ghosh, *Cogent Environ. Sci.*, 2017, **3**, 1401577.
46 J. A. García-Alonsoa and J. D. Real-Olverac, *Desalin. Water Treat.*, 2019, **162**, 331–340.
47 J. R. Araujo and B. S. Archanjo, *Biol. Fertil. Soils*, 2014, **50**, 1223–1232.
48 T. Pihlstrom, A. R. Fernandez-Alba, M. Gamon, C. F. Amate, M. E. Poulsen, R. Lippold, M. Anastassiades *Guidance document on analytical quality control and method validation procedures for pesticide residues and analysis in food and feed*, European Commission for Health And Food Safety, SANTE/12682/2019.
49 E. Smith, J. Smith, R. Naidu and A. L. Juhasz, *Water, Air, Soil Pollut.*, 2004, **151**, 71–86.
50 K. Thangavadivel, M. Megharaj, R. S. C. Smart, P. J. Lesniewski, D. Bates and R. Naidu, *Water, Air, Soil Pollut.*, 2011, **217**(1–4), 115–125.
51 B. Arunraj, T. Sathvika, V. Rajesh and N. Rajesh, *ACS Omega*, 2019, **4**, 940–952.
52 J. Kodali, S. Talasila, B. Arunraj and R. Nagarathnam, *Case Studies. Chem. Environ. Eng.*, 2021, **3**, 100099.
53 J. Kodali, B. Arunraj, T. Sathvika, A. S. K. Kumar and R. Nagarathnam, *RSC Adv.*, 2021, **11**, 22640–22651.